

# Leptonic $CP$ Violation and Proton Decay in $SUSY$ $SO(10)$

---

**Rabindra N. Mohapatra and Matt Sevrerson**

*Maryland Center for Fundamental Physics and Department of Physics, University of Maryland, College Park, Maryland 20742, USA*

**ABSTRACT:** We study the correlation between proton lifetime and leptonic  $CP$  violation in a class of renormalizable supersymmetric  $SO(10)$  grand unified theories (GUTs) with **10**, **126** and **120** Higgs fields, which provides a unified description of all fermion masses and possibly resolution of the strong  $CP$  problem. This specific model is unique in that it can readily be compatible with current proton lifetime limits for a supersymmetry (SUSY) breaking scale as low as 5 TeV due to the presence of a specific Yukawa texture. Our investigation here reveals that proton partial lifetimes predicted by this class of models will be tested by forthcoming proton decay searches; furthermore, a discovery of leptonic  $CP$  violation in neutrino oscillations would also lead to substantial reduction of the parameter space of the model.

---

## Contents

<b>1</b>	<b>Introduction</b>	<b>1</b>
<b>2</b>	<b>Details of the Model</b>	<b>4</b>
<b>3</b>	<b>CP Violation, Strong CP, and Yukawa Texture</b>	<b>5</b>
3.1	CP Violation and Potential Solution to Strong CP	5
3.2	CP Violation from Vacuum CP Phase	6
3.3	Parameter counting	7
<b>4</b>	<b>Proton Decay in the Model</b>	<b>8</b>
4.1	Dressed Operators	9
4.2	Rotation to Mass Basis	12
4.3	Proton Decay Width	13
<b>5</b>	<b>Fermion Fitting and Leptonic CP Violation</b>	<b>15</b>
5.0.1	Numerical Methods.	15
5.0.2	A Note on Threshold Corrections.	16
5.1	Fit Results for Type I Seesaw	17
5.1.1	Raw Couplings contributing to Proton Decay	19
5.2	Fit Results for Type II Seesaw	19
<b>6</b>	<b>Proton Lifetime Correlation with Dirac CP Phase</b>	<b>22</b>
6.1	Proton Partial Lifetimes for Type I Seesaw	23
6.2	Proton Partial Lifetimes for Type II Seesaw	24
<b>7</b>	<b>Summary and Conclusion</b>	<b>25</b>

---

## 1 Introduction

One of the major challenges for beyond the standard model physics is finding a unified understanding of all fermion masses including neutrinos. The origin and pattern of neutrino masses and mixings observed in various oscillation experiments over the past two decades not only reveals an absolute scale for neutrino masses substantially smaller than other fermions but also a leptonic mixing pattern quite different from the quarks. While the seesaw mechanism [1] is supposed to provide a simple path to the resolution of the scale problem, the problem of mixing is more complicated, and some believe that could be signal of new leptonic symmetries [2]. In particular as experiments make progress toward answering all remaining questions in neutrino mass physics, such as the type of mass hierarchy, presence of CP violation, and Dirac vs Majorana nature, it is important to

sharpen the predictions of various theories of neutrino masses, so that a clearer picture of the direction of physics beyond the standard model can be determined.

Grand unified theories [3] are a surprisingly appropriate setting for the seesaw mechanism for a number of reasons: (i) SO(10) theories [4] have  $B - L$  as a subgroup, which is naturally associated with the seesaw scale; (ii) the matter spinor of SO(10) automatically contains the right-handed neutrino field as a symmetry partner to the quarks and leptons of the standard model; (iii) SO(10) theories relate the Dirac mass of neutrinos to the up-like quark masses, leading to a seesaw scale near the GUT scale, which connects it to the scale of coupling unification as well.

In this paper, we discuss one class of supersymmetric SO(10) grand unified models including neutrinos and based on renormalizable Yukawa interactions [5–8]. The constraints of grand unification for this particular class are strong enough to make the model quite predictive in the fermion sector, due to fewer parameters in the Yukawa couplings [5]. For this class of models, we continue the exploration from previous work [17, 18] with the goal of extracting predictions for CP violation in neutrino oscillation and corresponding predictions for proton decay that can be used to test them.

As is well known, in SO(10) models, the fermions of each generation are assumed to reside in the **16**-dimensional spinor representation, and there are three kinds of Higgs field representations that can give renormalizable Yukawa couplings to generate fermion masses:  $\mathbf{10} \equiv H$ ,  $\overline{\mathbf{126}} \equiv \bar{\Delta}$  and  $\mathbf{120} \equiv \Sigma$ . The  $\bar{\Delta}$ -field is also used also to break the  $B - L$  gauge symmetry of the model, and since it breaks  $B - L$  by two units, this preserves discrete R-parity symmetry [9], leading to a [naturally stable lightest SUSY partner. Within this general framework, two kinds of renormalizable models have been discussed in the literature: (I) One that uses only  $\mathbf{10} + \overline{\mathbf{126}}$  Higgs superfields to give mass to the fermions which reside in the **16**-dim spinor representations of SO(10) [5, 6] and (II) another that uses all three representations, *i.e.*  $\mathbf{10} + \overline{\mathbf{126}} + \mathbf{120}$  [7, 8]. The GUT symmetry is broken by a subset of **210** ( $\Phi$ ), **45** ( $A$ ), **54** ( $S$ ) fields, which do not affect the fermion predictions. The first class of models with only **210** to break GUT symmetry was suggested early on as a minimal SUSY SO(10) class with coupling unification [10]. Both these classes provide a relatively economical way to fit all fermion masses and mixings, including neutrinos as well as quarks and charged leptons, and lead to predictions such as (i) normal hierarchy for neutrinos, (ii)  $\theta_{13}$  in agreement with observation [11], and (iii) CP violating phases for leptons, using a combination of both type I and type II seesaw [12].

What is in some sense amazing about this class of models is that despite the fact the quarks and leptons are unified, the diverse mixing patterns among them emerge without fine tuning. Especially in models that use  $\mathbf{10} + \overline{\mathbf{126}}$  fields for mass generation and where type II seesaw is assumed to dominate, an elegant explanation of the correct mixings emerges from the dynamical reason that in simple grand unified theories, bottom quark and tau lepton masses, become very close to each other when run up to the GUT scale [13]. This feature plays an important role in generating correct neutrino mixings in the general renormalizable SO(10) models as well.

Successes of these models in the fermion sector, as well as their economy, have led to further scrutiny of other model predictions accessible by experiment. Primary among such

tests is the classic prediction of proton decay in grand unified theories and the corresponding question of proton lifetime [14]. An advantage of renormalizable SUSY SO(10) models is that the same parameters that go into obtaining fermion mass fits also contribute to proton decay so that neutrino mixing angles and CP violating phases are expected to be correlated with proton lifetime, making it possible to test the models using measurements of those parameters together with those of proton lifetime.

This has been investigated in the framework of models with only  $\mathbf{10} + \overline{\mathbf{126}}$  Higgs superfields contributing to fermion mass, and there seems to be tension with current data [15, 16] unless the SUSY breaking scale is made high to suppress the  $d = 5$  contribution to p-decay amplitude. In fact it has been shown in [16] that the current limit on the mode  $p \rightarrow K^+ \nu$  implies a lower limit on the SUSY breaking scale of  $M_{susy} \geq 238$  TeV, which is much higher than the conventionally assumed value. Indeed, if any evidence for supersymmetry appears at the LHC energies, the  $\mathbf{10} + \overline{\mathbf{126}}$  will be ruled out.

It was suggested in [17] that with a choice of specific Yukawa textures, possible only in models with  $\mathbf{10} + \overline{\mathbf{126}} + \mathbf{120}$  due to fermion fit constraints, one can accommodate the proton lifetime bounds while keeping  $M_{susy}$  in the low TeV range. Detailed investigation of proton decay predictions of this model with  $M_{susy} \sim 5$  TeV was carried out in [18], and the results were found to be promising. The Dirac CP violating phase however was found to be  $\delta_{CP} \sim -7^\circ$  for the type II case, while the type I fit yielded a value of  $\delta_{CP} \sim -46^\circ$  [18]. Meanwhile, the NOVA and T2K results are providing hints of a larger  $\delta_{CP}$  [19].

In this paper, we discuss three new points beyond the analysis in Ref. [18]: (i) we explore a much wider domain of parameter space to see if the model can accommodate larger CP phase. We answer this question in the affirmative for the type I seesaw case and in the negative for type II case. (ii) We show how the CP phase predictions are correlated with predictions for proton lifetime. We believe that this result should be interesting since it is a primary goal of several planned experiments [20–23] to search for both proton decay and leptonic CP violation, which will then put this interesting class of models “under the microscope.” (iii) We also discuss how models of this type can provide a solution to the strong CP problem in a grand unified theory context without the need for an axion. On this point, we only show the result at the tree level and leave detailed investigation of any loop effects to a separate investigation.

Our calculation procedure is as follows: using the fermion mass sum rules predicted by these models, we calculate the GUT scale masses and mixings for the quarks and leptons and, through minimization of  $\sum \chi^2$ , attempt to locate fits to fermion sector measurements with CP phase outputs spanning the range of possible values. We create plots from the output data to observe which CP phase values are most favorable for the model. We then use the fermion fit data and varied values for the parameters of the proton decay operators (both LLLL and RRRR modes) to determine the  $p \rightarrow K^+ \bar{\nu}$  partial lifetime corresponding to each value for the CP phase, which illuminates whether phase values favored by the fermion sector are also consistent with proton lifetime constraints. We take gaugino masses to be 300 GeV and squark masses to be 5 TeV, although current data does not require us to use such high values. Predictions for lower SSB parameters can be easily obtained using scaling. The results we report can be used to test the model with the forthcoming

experiments [20–23].

This paper is organized as follows: in Sec. 2 we review the salient features of the model; Sec. 3 is devoted to a discussion of how CP violation is introduced into this model, and how our approach hints at a new way to solve the strong CP problem; in Sec. 4 we discuss proton decay operators in the model; Sec. 5 is devoted to fermion mass fitting and CP phase predictions in the model; and in Sec. 6, we present our predictions for proton lifetime and its correlation with the Dirac CP phase. Sec. 7 gives discussion and conclusion.

## 2 Details of the Model

The supersymmetric  $SO(10)$  model we consider has **10**-,  $\overline{\mathbf{126}}$ -, and **120**-dimensional Higgs fields with renormalizable Yukawa couplings contributing to fermion masses. The fields are named here as  $H$ ,  $\overline{\Delta}$ , and  $\Sigma$ , respectively. The relevant Yukawa superpotential terms are

$$W_Y \ni h_{ij} \Psi_i \Psi_j H + f_{ij} \Psi_i \Psi_j \overline{\Delta} + g_{ij} \Psi_i \Psi_j \Sigma, \quad (2.1)$$

where  $\Psi_i$  is the **16**-dimensional matter spinor containing superfields of all the SM fermions (of one generation) plus the right-handed neutrino, and  $i$  is the generation index. Additional multiplets such as **126**( $\Delta$ ), **210**( $\Phi$ ) and **54**( $S$ ) are needed to break the GUT symmetry and maintain supersymmetry below the GUT scale down to TeV scale. They contain in their decompositions color triplets that contribute to proton decay, as well as  $SU(2)$  doublets that contribute to the effective MSSM Higgs doublets, but they do not contribute to fermion masses.

All the doublets contained in the decompositions of  $H$ ,  $\overline{\Delta}$ ,  $\Sigma$ , and the other GUT-scale Higgs fields mix with each other in the mass matrix  $\mathcal{M}_{\mathcal{D}}$  defined by  $\varphi_u^T \mathcal{M}_{\mathcal{D}} \varphi_d$ , which is diagonalized by the bi-unitary rotation  $\mathcal{U} \mathcal{M}_{\mathcal{D}} \mathcal{V}^T$ . One linear combination each of the  $\varphi_{u,d}$  fields becomes the nearly massless MSSM Higgs doublet  $H_{u,d}$ , while the other combinations remain heavy. For  $H_{u,d}$  to remain light, the condition  $\det \mathcal{M}_{\mathcal{D}} \sim 0$  is necessary.

The full details of the mass matrices in terms of GUT-scale vevs and parameters are given for this type of model in [24]. The resulting effective Dirac fermion mass matrices can be written as [7]

$$\begin{aligned} \mathcal{M}_u &= \tilde{h} + r_2 \tilde{f} + r_3 \tilde{g} \\ \mathcal{M}_d &= \frac{r_1}{\tan \beta} (\tilde{h} + \tilde{f} + \tilde{g}) \\ \mathcal{M}_e &= \frac{r_1}{\tan \beta} (\tilde{h} - 3\tilde{f} + c_e \tilde{g}) \\ \mathcal{M}_{\nu_D} &= \tilde{h} - 3r_2 \tilde{f} + c_\nu \tilde{g}, \end{aligned} \quad (2.2)$$

with  $\tan \beta = v_u/v_d$ , where  $v_{u,d}$  are vevs of the MSSM fields  $H_{u,d}$ . For  $\lambda = h, f, g$ , the couplings  $\tilde{\lambda}_{ij}$  are related to  $\lambda_{ij}$  from eq. (2.1) by [17]

$$\tilde{h} \equiv \mathcal{V}_{11} h v_u; \quad \tilde{f} \equiv \frac{\mathcal{U}_{14} f v_u}{r_1 \sqrt{3}}; \quad \tilde{g} \equiv \frac{\mathcal{U}_{12} + \mathcal{U}_{13}/\sqrt{3}}{r_1} g v_u, \quad (2.3)$$

where  $1/\tan\beta$  takes  $v_u \rightarrow v_d$  for down-type fields; the vev ratios  $r_i$  and  $c_\ell$  are given by

$$\begin{aligned} r_1 &\equiv \frac{\mathcal{U}_{11}}{\mathcal{V}_{11}}; & r_2 &\equiv r_1 \frac{\mathcal{V}_{15}}{\mathcal{U}_{14}}; & r_3 &\equiv r_1 \frac{\mathcal{V}_{12} - \mathcal{V}_{13}/\sqrt{3}}{\mathcal{U}_{12} + \mathcal{U}_{13}/\sqrt{3}}; \\ c_e &\equiv \frac{\mathcal{U}_{12} - \mathcal{U}_{13}\sqrt{3}}{\mathcal{U}_{12} + \mathcal{U}_{13}/\sqrt{3}}; & c_\nu &\equiv r_1 \frac{\mathcal{V}_{12} + \mathcal{V}_{13}\sqrt{3}}{\mathcal{U}_{12} + \mathcal{U}_{13}/\sqrt{3}}, \end{aligned} \quad (2.4)$$

The full neutrino mass matrix is determined by both Majorana mass terms in the superpotential and the Dirac mass contribution given in eq. (2.2). The light masses can be generally given by a combination of the type-I and type-II seesaw mechanisms, involving the vevs of both left- and right-handed Majorana terms:

$$\mathcal{M}_\nu = v_L f - \mathcal{M}_{\nu_D} (v_R f)^{-1} (\mathcal{M}_{\nu_D})^T, \quad (2.5)$$

where  $v_{L,R}$  are the vevs of the SM-triplet  $\bar{\Delta}_L$  and singlet  $\bar{\Delta}_R$ , respectively, in **126**. We will separately consider cases of type-II ( $v_L$  term) and type-I ( $1/v_R$  term) dominance. Note that the presence of the  $f$  coupling in both terms intimately connects the neutrino mass matrix properties to those of the charged sector matrices, making the model quite predictive. Also note we will consider only normal mass hierarchy in this analysis, which arises naturally in this class of models.

### 3 CP Violation, Strong CP, and Yukawa Texture

In our phenomenological analysis, we will assume that  $\tilde{h}$ ,  $\tilde{f}$  are real and  $\tilde{g}$  is imaginary. Note that in the original model of this type with **120**, we could always choose  $h_{ii}$  to be real, but to make  $f_{ij}$  real and  $g_{ij}$  imaginary, we have to rely on some extra assumptions. We could view this choice simply as a way to fit observations; however, we argue below that this choice for the mass matrix parameters could arise from an underlying symmetry of the theory. We discuss two potential paths to obtaining CP violation naturally, and find that one of the ways could provide a path to resolution of the strong CP problem without the need for an axion. We show that in this case, the  $\theta$ -parameter is zero only at the tree level due to Hermiticity of the quark mass matrices; we defer a detailed discussion of this issue to a latter paper.

#### 3.1 CP Violation and Potential Solution to Strong CP

In this subsection we discuss the first approach to CP violation in the model. First we assume that theory is invariant under CP transformation of the fields as seen in Table 1, so that CP is spontaneously broken.

We supplement this transformation with a  $Z_2$  symmetry under which only the  $\Delta(126)$  field is odd while all other fields are even. Invariance under this symmetry implies that Yukawa couplings  $h, f$  are real and  $g$  is imaginary. After GUT symmetry breaking, one linear combination of the SM Higgs doublet fields remains massless, and it contains no

Field	CP transform
$\Psi(16)$	$\Psi^*(16)$
$H(10)$	$H^*(10)$
$\bar{\Delta}(\bar{126})$	$\bar{\Delta}^*(\bar{126})$
$\Delta(126)$	$-\Delta^*(126)$
$\Sigma(120)$	$-\Sigma^*(120)$
$A(45)$	$-A^*(45)$
$S(54)$	$S^*(54)$
$X(1)$	$X^*(1)$

**Table 1.** CP transformations of the superfields of the theory in the first approach.

complex parameters. To see this, first note that we do not have a **210** Higgs superfield in the theory. The superpotential for the symmetry breaking sector can then be written as:

$$\begin{aligned}
\mathcal{W} = & \sum_{\varphi} M_{\varphi} \varphi^2 + \lambda_1 X (A^2 - M_U^2) + \lambda_2 \Sigma A H + \\
& \frac{\lambda_3}{\Lambda} \bar{\Delta} A^2 H + \lambda_5 S A A + \lambda_6 S H H + \frac{1}{\Lambda} (\Delta \bar{\Delta})^2 \\
& + \lambda_7 S \Delta \Delta + \lambda_8 S \bar{\Delta} \bar{\Delta}
\end{aligned} \tag{3.1}$$

with  $\varphi = H, \Sigma, A, S$ .

Note that all superpotential parameters are real, and therefore we expect all resulting vevs to be real; furthermore, no new phases are expected to “sneak” in during the process of deriving the low-energy effective Lagrangian. After breaking the SM symmetry by the vevs of the Higgs fields (expected to be real), the resulting quark mass matrices are Hermitian at tree level and therefore have  $\text{Arg}(\text{Det } M_q) = 0$ , which gives no contribution to the strong CP phase  $\theta$  at tree level; additionally, due to reality of all the parameters in the superpotential, all heavy colored fermions also have real masses, so there is no contribution to the tree-level from them either. Thus at tree level  $\theta = 0$  at the GUT scale [25], and the model has the potential to give a solution for the strong CP problem without the need for an axion.

The loop effects (or RGE effects) on  $\theta$  are currently under study and are beyond the scope of this paper; for now we simply use this result to justify our choice for the form of the Yukawa couplings.

### 3.2 CP Violation from Vacuum CP Phase

A second approach to CP violation is to assume that the theory is again invariant under  $CP \times Z_2$ , but instead all fields transform as  $\Phi \rightarrow \Phi^*$  under CP. This implies that the matrices  $h$  and  $f$  are real and symmetric matrices and  $g$  is real and anti-symmetric. In this case, the **45** field  $A$  responsible for GUT symmetry breaking gets an *imaginary vev* via the F-term of a singlet  $X$ , through the superpotential term  $\lambda X (A^2 + M_U^2)$  (note the change of sign within the bracket compared to the corresponding term in eq. (3.1)). This imaginary

vev leads to an imaginary mixing term between the doublets  $H_{u,d}$  and  $\Sigma_{u,d}$  from **10** and **120**, respectively. Then, by redefining the doublets in **120** by  $\Sigma_{u,d} \rightarrow i\Sigma_{u,d}$  and keeping all other fields as they are, the effective Yukawa coupling of **120** doublets to matter fields becomes imaginary, whereas all other Yukawa couplings remain real. Below the GUT scale, the two linear combinations that become the MSSM doublets have all coefficients real since their mass matrices are real. In the language of mixings  $\mathcal{U}_{ij}$ , one sees that  $\mathcal{U}_{12,13}$  and  $\mathcal{V}_{12,13}$  are imaginary and all other elements real. Whether this case is also a potential solution to strong CP is not clear due to the color triplet fields having also imaginary coefficients after redefinition.

### 3.3 Parameter counting

With either of the above choices of symmetry, and in the absence of any texture assumptions, the mass matrices for the fermions are now Hermitian and contain a total of 12 parameters from Yukawa couplings; seven additional parameters from doublet vevs, including  $v_L$  in the type-II contribution, bring the total number of parameters to 18; finally, three more parameters arise once we account for threshold effects, bringing the total to 21.

To reduce the number of parameters, and also to ameliorate the proton decay problem of these models, we consider the reduced Yukawa texture proposed and analyzed in [17] and further studied in [18]. The proposed [17] texture has the form

$$\begin{aligned}\tilde{h} &= \begin{pmatrix} 0 & & \\ & 0 & \\ & & M \end{pmatrix}, & \tilde{f} &= \begin{pmatrix} \sim 0 & \sim 0 & \tilde{f}_{13} \\ \sim 0 & \tilde{f}_{22} & \tilde{f}_{23} \\ \tilde{f}_{13} & \tilde{f}_{23} & \tilde{f}_{33} \end{pmatrix}, \\ \tilde{g} &= i \begin{pmatrix} 0 & \tilde{g}_{12} & \tilde{g}_{13} \\ -\tilde{g}_{12} & 0 & \tilde{g}_{23} \\ -\tilde{g}_{13} & -\tilde{g}_{23} & 0 \end{pmatrix},\end{aligned}\tag{3.2}$$

where we note that  $\tilde{h}$  is an explicitly rank-1 matrix, with  $M \sim m_t$ ; thus, at first order, the **10** Higgs contributes to the third generation masses and nothing more.

The above matrices have 10 parameters (with  $f_{11}$  and  $f_{12}$  small but nonzero and not shown in the above equation), so taken in combination with  $v_L$  and the vev mixing ratios  $r_i$  and  $c_\ell$ , the model has a total of 16 parameters. Correspondingly, there are 18 measured parameters associated with the physical fermions, with limits on the Dirac CP phase in the PMNS matrix beginning to materialize. Hence, we would like to predict 19 observables in the fermion sector. The model is surprisingly close to fitting all 19 values with its 16 parameters, but ultimately the inclusion of SUSY threshold corrections, which provides three additional parameters (expected to be significant for large  $\tan\beta$ ), are needed to get a good fit [26]; they provide the model with the three additional degrees of freedom needed to accommodate all 19 observables, without tension from squark and Higgs mass constraints in the MSSM sectors [26] [18].

Note that the magnitude constraints on the  $f_{ij}$  and  $g_{ij}$  required by the texture ansatz, as well as phenomenological constraints on the threshold corrections [26], prevent a true



$\sum \chi^2 = 0$  fit to the data despite the sufficient naive match between input and output counts.

#### 4 Proton Decay in the Model

The baryon-number violating operators leading to proton decay with which we are concerned in this paper follow from the presence of  $SU(3)$  color-triplets  $(\mathbf{3}, \mathbf{1}, -\frac{1}{3}) + \text{c.c.}$  in the decompositions of the GUT Higgs fields; these triplets mix with each other in a mass matrix  $\mathcal{M}_T$ , which is diagonalized by the bi-unitary rotation  $\mathcal{X} \mathcal{M}_T \mathcal{Y}^T$ . Two exotic types of triplets also lead to  $B$ - or  $L$ -violating vertices,  $(\mathbf{3}, \mathbf{1}, -\frac{4}{3}) + \text{c.c.}$ , which interact with two up-type or two down-type RH singlet fermions, and  $(\mathbf{3}, \mathbf{3}, -\frac{1}{3}) + \text{c.c.}$ , with a pair of LH doublets. The exotic triplets mix in their own respective  $(2 \times 2)$  matrices. All such triplets are expected to be heavy with masses near the GUT scale.

Exchange of conjugate pairs of any of these triplets leads to operators that change two quarks into an anti-quark and a lepton; such operators are numerically dominant over the corresponding exchange of the scalar superpartners of these triplets, and may be so over gauge boson exchange as well. Figure 1 shows Feynman diagrams for two examples of the operators in question.

The corresponding  $d = 5$  effective superpotential is

$$\mathcal{W}_{\Delta B=1} = \frac{\epsilon_{abc}}{M_T} \left( \hat{C}_{ijkl}^L Q_i^a Q_j^b Q_k^c L_l + \hat{C}_{[ijk]l}^R U_i^c D_j^b U_k^c E_l \right), \quad (4.1)$$

where  $i, j, k, l = 1, 2, 3$  are the generation indices and  $a, b, c = 1, 2, 3$  are the color indices. This potential has  $\Delta L = 1$  in addition to  $\Delta B = 1$  and so also has  $\Delta(B - L) = 0$ .  $M_T \sim M_U$  is a generic GUT-scale mass for the triplets. The left-handed term expands to

$$\mathcal{W}_{\Delta B=1} \ni \frac{\epsilon_{abc}}{M_T} \left( \hat{C}_{\{ij\}kl}^L U_i^a D_j^b U_k^c E_l - \hat{C}_{\{i[j\}k\}l}^L U_i^a D_j^b D_k^c \mathcal{N}_l \right), \quad (4.2)$$

where  $\mathcal{N}$  is the left-handed neutrino superfield. The anti-symmetrizing of indices in the  $C_R$  operator from (4.1) and here in the  $C_L$  reflects the non-vanishing contribution from the contraction of the color indices. The symmetrization in  $i, j$  in the  $C_L$  comes as a result of the doublet contractions.

The effective operator coefficients  $C_{ijkl}$  are of the form

$$C_{ijkl}^L = \sum_a \left( \mathcal{X}_{a1} h + \mathcal{X}_{a4} f + \sqrt{2} \mathcal{X}_{a3} g \right)_{ij} (\mathcal{Y}_{a1} h + \mathcal{Y}_{a5} f)_{kl} + \text{exotic terms}; \quad (4.3)$$

$$C_{ijkl}^R = \sum_a \left( \mathcal{X}_{a1} h - \mathcal{X}_{a4} f + \sqrt{2} \mathcal{X}_{a2} g \right)_{ij} \left[ \mathcal{Y}_{a1} h - \left( \mathcal{Y}_{a5} - \sqrt{2} \mathcal{Y}_{a6} \right) f + \sqrt{2} (\mathcal{Y}_{a3} - \mathcal{Y}_{a2}) g \right]_{kl} + \text{exotic terms} \quad (4.4)$$

where the matrices  $\mathcal{X}$  and  $\mathcal{Y}$  are those that diagonalize the triplet mass matrix; hence elements of those matrices will be between 0 and 1. These elements are algebraic combinations of the various GUT scale masses and couplings; again the details of their properties can be seen in [24]. Nearly all such parameters are essentially unconstrained and can be

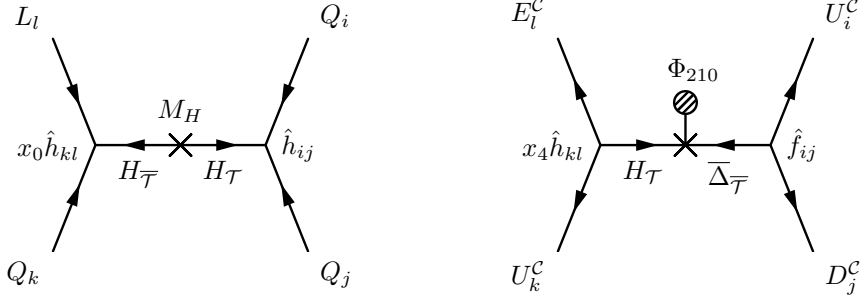


**Figure 1.** Examples of superfield diagrams that lead to proton decay in this model. The hats on the couplings indicate mass basis, and the parameters  $x_i$  contain the triplet mixing information unique to the specific pairing of couplings present in each diagram (see below).

taken as arbitrary for the purposes of our analysis. The one exception here is the product  $\mathcal{X}_{a1}\mathcal{Y}_{a1} \sim M_H$ , which is fixed by the tuning condition for  $M_{\mathcal{D}}$  discussed above. As a result, the value of this product needs to be generally  $\mathcal{O}(1)$ .

Due to the largely unconstrained nature of the remaining parameters, it is typical to re-cast the  $C_{ijkl}$  coefficients in the following parametrization:

$$\begin{aligned}
C_{ijkl}^L &= x_0 h_{ij} h_{kl} + x_1 f_{ij} f_{kl} - x_3 h_{ij} f_{kl} - x_4 f_{ij} h_{kl} + y_5 f_{ij} g_{kl} + y_7 h_{ij} g_{kl} \\
&\quad + y_9 g_{ik} f_{jl} + y_{10} g_{ik} g_{jl}, \\
C_{ijkl}^R &= x_0 h_{ij} h_{kl} + x_1 f_{ij} f_{kl} + x_2 g_{ij} g_{kl} + x_3 h_{ij} f_{kl} + x_4 f_{ij} h_{kl} + x_5 f_{ij} g_{kl} \\
&\quad + x_6 g_{ij} f_{kl} + x_7 h_{ij} g_{kl} + x_8 g_{ij} h_{kl} + x_9 f_{il} g_{jk} + x_{10} g_{il} g_{jk},
\end{aligned} \tag{4.5}$$

where  $x_0 \equiv \mathcal{X}_{a1}\mathcal{Y}_{a1} \sim 1$ . Note that several identifications have already been made here:  $y_{0,1} = x_{0,1}$  and  $y_{3,4} = -x_{3,4}$ ; the would-be parameters  $y_{2,6,8} = 0$ . The parameters  $x_{9,10}$  and  $y_{9,10}$  correspond to the exotic triplets; the indices of those terms are connected in unique ways as a result of the distinct contractions of fields.

The couplings  $h, f, g$  as written correspond to matter fields in the flavor basis and undergo unitary rotations in the change to mass basis, as indicated by the hats on  $\hat{C}^{L,R}$  in eqs. (4.1) and (4.2) above. For more general Yukawa textures, this change of basis does not alter the prescription significantly, and so the corresponding rotations are often overlooked in similar analyses; for this work however the rank-1 nature of the **10** coupling results in an increased sensitivity to the basis change, and so it cannot be safely ignored. I will return to the details of the pertinent rotations in basis after introducing the contributing operators.

#### 4.1 Dressed Operators

The pertinent superfield operators are realized at leading order through conjugate pairs of Higgsino triplet mediators, and the outgoing squarks and sleptons interact with gauginos or (SUSY) Higgsinos to produce the corresponding outgoing fermions, as seen in Figure 2. The resulting  $d = 6$  effective operators have the four-fermion form needed to enable proton decay.

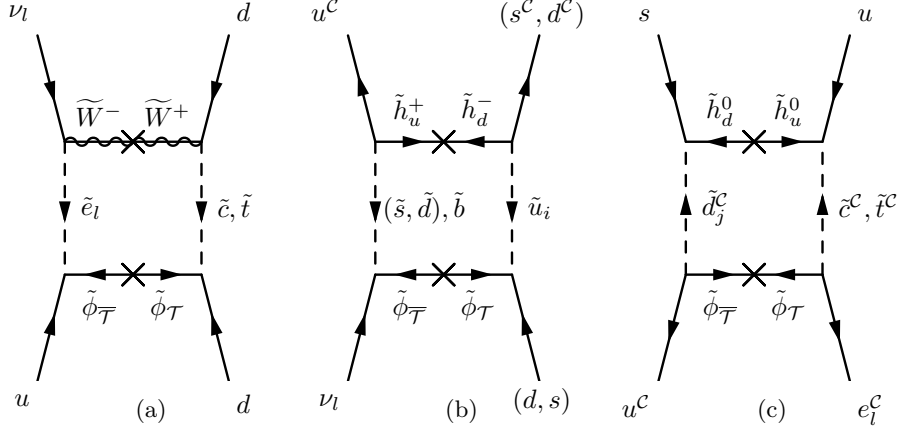


**Figure 2.** Examples of dressed diagrams leading to proton decay in the model. Diagram (a) shows a contribution to  $p \rightarrow \pi^+ \bar{\nu}_l$ ; integrating out the triplets gives an effective operator of type  $C^L u d u e$ . Diagram (b) shows a  $C^L u d d \nu$ -type operator contributing to  $K^+ \bar{\nu}_l$ . Diagram (c) shows a  $C^R u^C d^C u^C e^C$ -type operator contributing to  $K^0 e_l^+$ , for  $l = 1, 2$ . Note where more than one field is listed, each choice gives a separate contributing channel, except for the dependent exchange of  $(s \leftrightarrow d)$  in (b).

Depending on the sfermions present, diagrams may in principle be dressed with gluinos, Winos, Binos, or Higgsinos.<sup>1</sup> Gluino, Bino, and  $\widetilde{W}^0$  operators can contribute to only the  $p \rightarrow K^+ \bar{\nu}_l$  mode, through the  $UDSN$  operator (left-handed only), due to generation diagonality of the interactions and generation anti-symmetry of the quarks in the  $C_{ijkl}$ . Furthermore, those contributions from gluino- and Bino-dressed operators vanish by Fierz identity under the universality assumption [18].

Charged Wino and both charged and neutral Higgsinos contribute to significantly more channels due to the possibility for generation-mixing through unitary matrix and Yukawa factors, respectively, although they come at the price of suppression from off-diagonal elements of pairs of those factors, *e.g.*  $U_{k2}^d U_{l1}^u$  or  $y_{l1}^u y_{l1}^d$ . However, the sparse or hierarchical texture of the GUT Yukawas leads to a very large spread in the magnitudes of the  $C_{ijkl}$  values, and so there is no general dominance of the operators without such suppression factors over those with them.

Higgsino-dressed operators will generally contribute through both left- and right-handed channels, and interference is present among any group with all external legs of matching chiralities. Because we are deliberately choosing large  $\tan \beta$  to examine the most general scenario, there is no overall suppression of right-handed operators present in the analysis. Hence, we will make no *a priori* assumptions about the significance of their contributions, and have rather examined all contributions explicitly.

Two remaining restrictions that apply here are: (a) since the mass terms for the  $W$

<sup>1</sup>We give this discussion in terms of  $\widetilde{B}$ ,  $\widetilde{W}^0$ , and  $\tilde{h}_{u,d}^{\pm,0}$ , rather than  $\tilde{\chi}^\pm$  and  $\tilde{\chi}_i^0$ , because (a) we assume universal mass spectrum for superpartners to satisfy FCNC constraints, meaning the mass and flavor eigenstates coincide for the gauge bosons, and (b) chargino and neutralino masses differ from  $M_{SUSY}$  by  $\mathcal{O}(1)$  factors as long as gaugino soft masses are relatively small compared to  $M_{SUSY}$ . These assumptions simplify computations with little affect on the numerical factors.

and the SUSY Higgs couple  $W^+$  to  $W^-$  and  $H_u$  to  $H_d$ , one will not see contributions from triplet operators with sfermions of like  $SU(2)$  flavor, and (b) one will not see the triplet operator  $\tilde{u}du\tilde{e}$  dressed by  $\tilde{h}^\pm$  nor  $u\tilde{d}d\tilde{\nu}$  dressed by  $\tilde{h}^0$  because each would result in an outgoing left-handed anti-neutrino.

We can write the operator for any pertinent decay mode as a generic Wino- or Higgsino coefficient times one of several flavor-specific sub-operators; the forms of the general operators are

$$\mathcal{O}_{\tilde{W}} = \left( \frac{i\alpha_2}{4\pi} \right) \left( \frac{1}{M_{\mathcal{T}}} \right) I(M_{\tilde{W}}, m_{\tilde{q}}) \mathcal{C}_{\tilde{W}}^A \quad (4.6)$$

and

$$\mathcal{O}_{\tilde{h}} = \left( \frac{i}{16\pi^2} \right) \left( \frac{1}{M_{\mathcal{T}}} \right) I(\mu, m_{\tilde{q}}) \mathcal{C}_{\tilde{h}}^A, \quad (4.7)$$

where<sup>2</sup>

$$I(a, b) = \frac{a}{b^2 - a^2} \left\{ 1 + \frac{a^2}{b^2 - a^2} \log \left( \frac{a}{b} \right) \right\},$$

and the sub-operators  $\mathcal{C}^A$  are, for the neutral Wino:<sup>3</sup>

$$\begin{aligned} \mathcal{C}_{\tilde{W}^0}^I &= \epsilon_{abc} (u^{T^a} C^{-1} s^c) \hat{C}_{1[12]l}^L (d^{T^b} C^{-1} \nu_l) \\ \mathcal{C}_{\tilde{W}^0}^{II} &= \epsilon_{abc} (u^{T^a} C^{-1} d^b) \hat{C}_{1[12]l}^L (s^{T^c} C^{-1} \nu_l) \end{aligned} \quad (4.8)$$

for the (charged) Wino:

$$\begin{aligned} \mathcal{C}_{\tilde{W}^\pm}^I &= \frac{1}{2} (u d_j) \hat{C}_{[ij1]l}^L U_{ii'}^d U_{ll'}^\nu (d_{i'} \nu_{l'}) \\ \mathcal{C}_{\tilde{W}^\pm}^{II} &= \frac{1}{2} (u e_l) \hat{C}_{[1jk]l}^L U_{kk'}^d U_{j1}^u (d_{k'} u) \\ \mathcal{C}_{\tilde{W}^\pm}^{III} &= -\frac{1}{2} (u d_k) \hat{C}_{1[jk]l}^L U_{j1}^u U_{ll'}^e (u e_{l'}) \\ \mathcal{C}_{\tilde{W}^\pm}^{IV} &= -\frac{1}{2} (d_j \nu_l) \hat{C}_{[ijk]l}^L U_{ii'}^d U_{k1}^u (d_{i'} u) \end{aligned} \quad (4.9)$$

for the charged Higgsino:

$$\begin{aligned} \mathcal{C}_{\tilde{h}^\pm}^I &= (u e_l) \hat{C}_{[1jk]l}^L y_{kk'}^{d\dagger} y_{j1}^{u\dagger} (d_{k'}^C u^C) \\ \mathcal{C}_{\tilde{h}^\pm}^{II} &= -(u d_k) \hat{C}_{1[jk]l}^L y_{j1}^{u\dagger} y_{ll'}^{e\dagger} (u^C e_{l'}^C) \\ \mathcal{C}_{\tilde{h}^\pm}^{III} &= -(d_j \nu_l) \hat{C}_{i[jk]l}^L y_{ii'}^{d\dagger} y_{k1}^{u\dagger} (d_{i'}^C u^C) \\ \mathcal{C}_{\tilde{h}^\pm}^{IV} &= (u^C d_j^C) \hat{C}_{[ij1]l}^R y_{ii'}^u y_{ll'}^e (d_{i'} \nu_{l'}) \\ \mathcal{C}_{\tilde{h}^\pm}^V &= (u^C e_l^C) \hat{C}_{[1jk]l}^R y_{kk'}^u y_{j1}^d (d_{k'} u) \end{aligned} \quad (4.10)$$

---

<sup>2</sup>One might notice that this expression for  $I(a, b)$  differs from what is usually given in the literature for analogous proton decay expressions; the discrepancy is due to inclusion of the universal mass assumption prior to evaluating the loop integral.

<sup>3</sup>We include the spinor and color details for the neutral Wino operators, but suppress them afterward.

and for the neutral Higgsino:

$$\begin{aligned}
\mathcal{C}_{\tilde{h}^0}^I &= -(u d_k) \hat{C}_{[ij1]l}^L y_{i1}^{u\dagger} y_{ll'}^{e\dagger} (u^C e_{l'}^C) \\
\mathcal{C}_{\tilde{h}^0}^{II} &= -(u e_l) \hat{C}_{[1jk]l}^L y_{kk'}^{d\dagger} y_{j1}^{u\dagger} (d_{k'}^C u^C) \\
\mathcal{C}_{\tilde{h}^0}^{III} &= (d_j \nu_l) \hat{C}_{i[jk]l}^L y_{i1}^{u\dagger} y_{kk'}^{d\dagger} (u^C d_{k'}^C) \\
\mathcal{C}_{\tilde{h}^0}^{IV} &= -(u^C d_j^C) \hat{C}_{[ij1]l}^R y_{i1}^u y_{ll'}^e (u e_l) \\
\mathcal{C}_{\tilde{h}^0}^V &= -(u^C e_l^C) \hat{C}_{[1jk]l}^R y_{k1}^u y_{jj'}^d (u d_{j'})
\end{aligned} \tag{4.11}$$

Again the hats on  $\hat{C}^{L,R}$  indicate  $\hat{h}, \hat{f}, \hat{g}$  are rotated to the mass basis, which I will discuss in detail shortly. Note that  $UDUE$  and  $UDDN$  operators generally differ by a sign, as do diagrams dressed by  $\tilde{h}_{u,d}^\pm$  and  $\tilde{h}_{u,d}^0$ . These sign differences lead to cancellations within the absolute squared sums of interfering diagrams, and even cancellation of entire diagrams with each other in some cases.

The corresponding Feynman diagrams for all non-vanishing channels for the  $K^+ \bar{\nu}_l$ ,  $K^0 \ell^+$ ,  $\pi^+ \bar{\nu}_l$ , and  $\pi^0 \ell^+$  modes are catalogued in the Appendix of [18]. All non-negligible contributions used here in the analysis are catalogued in Appendix B.

Note that since the SUSY Yukawas  $y^f$  present in the  $\mathcal{C}^A$  are not physically determined, we define approximations to the Yukawas by using weak scale masses rotated by GUT-scale  $U^f$  (which are determined by our fermion sector fitting):

$$y^u = \frac{1}{v_u} U_u \left( \mathcal{M}_u^{\text{wk}} \right)^D U_u^\dagger,$$

where  $v_u = v_{\text{wk}} \sin \beta$ , or, in component notation,

$$y_{ij}^u = \frac{1}{v_u} \sum_k m_k^u U_{ik}^u U_{jk}^{u*}, \tag{4.12}$$

with similar expressions for  $y^d$  and  $y^e$ .

We used mass values from the current PDG [28]; light masses were run to the 1-GeV scale, and top and bottom masses were taken on-shell.

Note that since the Yukawa factors always appear in pairs of opposite flavor in the Higgsino operators, and since  $\frac{1}{\sin \beta \cos \beta} \simeq \tan \beta$  for large  $\beta$ , the Higgsino contributions to proton decay  $\sim \frac{\tan^2 \beta}{v_{\text{wk}}^4}$  for this model.

## 4.2 Rotation to Mass Basis

There are generally two distinct mass-basis rotations possible for each of the  $UDUE$ -,  $UDDN$ -, and  $U^C D^C U^C E^C$ -type triplet operators; the difference between the two depends on whether the operator is “oriented” (*i.e.*, in the diagram) such that the lepton is a scalar. For a given orientation, a unitary matrix corresponding to the fermionic field at one vertex in the triplet operator will rotate every coupling present in  $C^{L,R}$  pertaining to that vertex; an analogous rotation will happen for the other vertex in the operator. For example, looking at the  $\pi^+ \bar{\nu}_l$  channel in Figure 2(a), every coupling  $\lambda_{ij}$  ( $\lambda = h, f, g$ ) from

$C_{ijkl}^L$  present at the  $\tilde{\phi}\mathcal{T}$  vertex will be rotated by  $U^d$ ; similarly all  $\kappa_{kl}$  present at the  $\tilde{\phi}\overline{\mathcal{T}}$  vertex will be rotated by  $U^u$ .

The down quark field shown is a mass eigenstate quark resulting from unitary the rotation, which we can interpret as a linear combination of flavor eigenstates:  $d_j = U_{jm}^d d'_m$ , with  $j = 1$ ; applying the same thinking to the up quark, we can also write  $u_k^T = u_p'^T U_{pk}^u$ , with  $k = 1$ . To work out the details of the rotations, we can start with the  $d = 5$  operator written in terms of flavor states<sup>4</sup>,  $\sum_a x_a (\tilde{u}_i \lambda_{im}^a d'_m) (u_p' \kappa_{pl}^a \tilde{e}_l)$ , where I have expanded  $C_{impl}^L$  in terms of its component couplings and chosen the indices with the malice of forethought; now we can write

$$\begin{aligned} & \sum_a x_a (\tilde{u}_i^T C^{-1} \lambda_{im}^a d'_m) (u_p'^T \kappa_{pl}^a C^{-1} \tilde{e}_l) \\ &= \sum_a x_a (\tilde{u}_i^T C^{-1} \underbrace{\lambda_{im}^a U_{mj}^{d\dagger}}_{\equiv \hat{\lambda}_{ij}^a} \underbrace{U_{jn}^d d'_n}_{d_j}) (\underbrace{u_p'^T U_{pk}^u}_{u_k^T} \underbrace{U_{kq}^{u*} \kappa_{ql}^a}_{\equiv \hat{\kappa}_{kl}^a} C^{-1} \tilde{e}_l). \end{aligned}$$

Using the new definitions for  $\hat{\lambda}$ , we can see that the rotated coefficient  $\hat{C}^L$  corresponding to the expression in eq. (4.5) has become

$$\begin{aligned} \hat{C}_{ijkl}^L &= x_0 \hat{h}_{ij} \hat{h}_{kl} + x_1 \hat{f}_{ij} \hat{f}_{kl} - x_3 \hat{h}_{ij} \hat{f}_{kl} + \dots \\ &= x_0 (h U_d^\dagger)_{ij} (U_u^* h)_{kl} + x_1 (f U_d^\dagger)_{ij} (U_u^* f)_{kl} - x_3 (h U_d^\dagger)_{ij} (U_u^* f)_{kl} + \dots \end{aligned} \quad (4.13)$$

Note that this version of  $\hat{C}^L$  is only valid for  $UDUE$ -type operators with this orientation in the diagram, namely, those with a scalar  $\tilde{e}$ ; there is an analogous pair of rotations for  $UDUE$  with a scalar down and fermionic lepton, as well as two each for  $UDDN$  and  $U^c D^c U^c E^c$ , for a total of six possible schemes.

### 4.3 Proton Decay Width

The full proton decay width  $\tau (p \rightarrow M\bar{\ell})$  (where  $M = K, \pi$  is the final meson state) can be written as

$$\Gamma = \frac{1}{4\pi} \beta_H^2 (A_L A_S)^2 (|\mathcal{O}_{\widetilde{W}}|^2 + |\mathcal{O}_{\widetilde{h}}|^2) p, \quad (4.14)$$

where

- $\mathcal{O}_{\widetilde{W}}$  and  $\mathcal{O}_{\widetilde{h}}$  are the operators given in (4.6) and (4.7).
- The Hadronic factor  $\beta_H^2$  is defined by  $\langle M | (qq)q | p \rangle \sim \beta_H P u_p$ ; the parameter is discussed extensively in works such as [30] and [31]; its value is now most commonly found in the range (0.006 - 0.03), with a tendency to prefer  $\beta_H \sim 0.015$ , as seen in [30]. We will take a slightly favorable approach and use  $\beta_H = 0.008$ .
- The factors  $A_L$  and  $A_S$  account for the renormalization of the  $d = 6$  dressed operators from  $M_p \rightarrow M_{SUSY}$  and  $M_{SUSY} \rightarrow M_U$ , respectively; their values have been calculated in the literature as  $A_L = 0.4$  and  $A_S = 0.9-1.0$  [33].

---

<sup>4</sup>Recall the scalars are both mass and flavor eigenstates under the universal mass assumption

- In the rest frame of the proton, the external momentum  $\mathbf{p} = |\mathbf{p}| \equiv -\mathbf{p}_M = \mathbf{p}_\ell$  is given by

$$\mathbf{p} \simeq \frac{M_p}{2} \left( 1 - \frac{m_M^2}{M_p^2} \right), \quad (4.15)$$

where we have assumed  $m_\ell^2 \ll |\mathbf{p}|^2$  (which is only marginally valid for  $m_\mu$  but clearly so for  $m_e$ ). Note that  $\mathbf{p} \sim M_p/2$  for pion modes, but that value is reduced by a factor of  $\sim 25\%$  for kaon modes.

Let us make one further definition to allow for clear statement of the working formulae for the partial decay widths of the proton. We define  $C^{\mathcal{A}}$  as extended forms of the  $C_{ijkl}$  by

$$\begin{aligned} \mathcal{C}_{\widetilde{W}}^{\mathcal{A}} &= C_{\widetilde{W}}^{\mathcal{A}}(qq)(q\ell) \\ \mathcal{C}_{\widetilde{h}}^{\mathcal{A}} &= C_{\widetilde{h}}^{\mathcal{A}}(qq)(q\ell) \end{aligned} \quad (4.16)$$

so that these coefficients contain the  $U^f$  or  $y^f$  factors as well as the  $C_{ijkl}$  of the  $\mathcal{C}^{\mathcal{A}}$  operators in (4.8)-(4.11). This gives us the ability to easily translate an operator expression like <sup>5</sup>

$$\mathcal{O}_{\widetilde{W}}(K^+\bar{\nu}) \simeq \left( \frac{i\alpha_2}{4\pi} \right) \frac{1}{M_{\mathcal{T}}} \left( \frac{M_{\widetilde{W}}}{m_{\widetilde{q}}^2} \right) \{ \mathcal{C}_{\widetilde{W}}^I + \mathcal{C}_{\widetilde{W}}^{IV} \} \quad (4.17)$$

into a partial decay width statement,

$$\Gamma_{\widetilde{W}}(p \rightarrow K^+\bar{\nu}) \simeq \frac{1}{4\pi} \left( \frac{\alpha_2}{4\pi} \right)^2 \frac{1}{M_{\mathcal{T}}^2} \left( \frac{M_{\widetilde{W}}}{m_{\widetilde{q}}^2} \right)^2 \beta_H^2 (A_L A_S)^2 \mathbf{p} \cdot |C_{\widetilde{W}}^I + C_{\widetilde{W}}^{IV}|^2, \quad (4.18)$$

without losing either information or readability. Hence, we can now present relatively compact and intelligible expressions for the Wino- and Higgsino-dressed partial decay widths of the proton for generic mode  $p \rightarrow M\bar{\ell}$ :

$$\Gamma_{\widetilde{W}}(p \rightarrow M\bar{\ell}) \simeq \frac{1}{4\pi} \left( \frac{\alpha_2}{4\pi} \right)^2 \frac{1}{M_{\mathcal{T}}^2} \left( \frac{M_{\widetilde{W}}}{m_{\widetilde{q}}^2} \right)^2 \beta_H^2 (A_L A_S)^2 \mathbf{p} \cdot \left| \sum_{\mathcal{A} \in M\bar{\ell}} C_{\widetilde{W}}^{\mathcal{A}} \right|^2 \quad (4.19)$$

$$\Gamma_{\widetilde{h}}(p \rightarrow M\bar{\ell}) \simeq \frac{1}{4\pi} \left( \frac{1}{16\pi^2} \right)^2 \frac{1}{M_{\mathcal{T}}^2} \left( \frac{\mu}{m_{\widetilde{q}}^2} \right)^2 \beta_H^2 (A_L A_S)^2 \mathbf{p} \cdot \left| \sum_{\mathcal{A} \in M\bar{\ell}} C_{\widetilde{h}}^{\mathcal{A}} \right|^2. \quad (4.20)$$

For the numerical analysis, we used the generic values

$$M_{\mathcal{T}} = 2 \times 10^{16} \text{ GeV}, \quad M_{\widetilde{W}} = \mu = 300 \text{ GeV}, \quad m_{\widetilde{q}} = 5 \text{ TeV}.$$

Like our choice for  $\tan \beta$ , these choices for  $\mu$  and  $m_{\widetilde{q}}$  are chosen to yield deliberately strict constraints in order to hold the model to the highest feasible scrutiny; *i.e.*, we are presenting the “worst case scenario” for the model.

Also, let us repeat here that because of the two SUSY Yukawa coupling factors in the  $C_{\widetilde{h}}^{\mathcal{A}}$ , which always come in opposite flavor,

$$\Gamma_{\widetilde{h}} \propto \left( \frac{1}{v_{\text{wk}}^2 \sin \beta \cos \beta} \right)^2 \sim \frac{\tan^2 \beta}{v_{\text{wk}}^4}.$$

---

<sup>5</sup>Here, we use the approximation  $I(M_{\widetilde{W}}, m_{\widetilde{q}}) \sim M_{\widetilde{W}}/m_{\widetilde{q}}^2$  for the loop integral factor.

Finally, note that because the Higgsino vertices change the chiralities of the outgoing fermions, there can be no interference between Wino- and Higgsino-dressed diagrams, as suggested by eq. (4.14); however, since diagrams for the right-handed  $C^R$  operators have outgoing *left-handed* fermions by the same Higgsino mechanism, diagrams for  $C^R$ - and  $C^L$ -type operators with the same external particles of matching chiralities *do* interfere with each other, and so all such contributions to a given mode do in fact go into the same absolute-squared sum factor, as suggested by eq. (4.20).

## 5 Fermion Fitting and Leptonic CP Violation

Our first computational goal with this model was to understand its preferences and flexibility in predicting a value for the neutrino sector CP phase for experimental agreement with all known fermion parameters. Because of the beginning trend in the data, we placed some focus on phase values in the large negative range, *i.e.* with  $\sin \delta_{\text{CP}} \sim 1$ ; however, given the current uncertainty in the measured value, we also wanted to consider the entire range of possibilities.

By diagonalizing the mass matrices given in eq. (2.2), with the Yukawa textures shown in (3.2), one can obtain the GUT-scale fermion masses and mixing angles for a given set of values for the mass matrix parameters  $h_{ij}$ ,  $f_{ij}$ ,  $r_i$ , etc. To find a best fit to the experimental data, we use the `Minuit` tool library for Python [34, 35] to minimize the sum of chi-squares for neutrino mass-squared differences  $\Delta m_{21}^2$  (aka  $\Delta m_{\odot}^2$ ) and  $\Delta m_{32}^2$  (aka  $\Delta m_{\text{atm}}^2$ ) and the PMNS mixing angles as well as the mass eigenvalues and CKM mixing angles in the charged-fermion sector.

### 5.0.1 Numerical Methods.

Because the input parameter space of the model is large and highly non-linear, and because our minimization tools depend on a measurement of the local gradient, our choices for initial values in any search are likely to affect the output results. In order to ensure a high likelihood for finding global minima, after setting some rough initial values for the inputs using analytical arguments, we use an iterative systematic approach in refining those values.

Furthermore, for this analysis, since we were interested in the full range of possibilities for the CP phase output, we chose multiple initial positions within the parameter space from which to perform our minimization. Our specific choices result in three distinct values for the CP phase while approximating the remaining fermion sector to a crude but sufficient degree for initialization.

The three initial inputs are given in Table 2.

From each starting position, we search for a series of potential fits by iteratively including a “target” value for the PMNS Jarlskog invariant from the interval  $J_{\nu} = [-0.03466, 0.03466]$ , which corresponds to the entire range of possible phase values  $-1 \leq \sin \delta_{\text{CP}} \leq 1$ . The target is implemented by including  $J_{\nu}$  in the sum of chi-squares for the outputs. Once the best fit is found, this hypothetical  $J_{\nu}$  contribution to the sum of chi-squares is subtracted out to obtain the true value for the fit.



	Init #1	Init #2	Init #3
$M$ (GeV)	80.2	76.1	79.0
$\tilde{f}_{11}$ (GeV)	0.0055	0.01013	0.0145
$\tilde{f}_{12}$ (GeV)	0.0965	-0.089	0.064
$\tilde{f}_{13}$ (GeV)	0.608	0.9397	1.55
$\tilde{f}_{22}$ (GeV)	1.094	0.866	1.32
$\tilde{f}_{23}$ (GeV)	1.21	1.4884	-0.75
$\tilde{f}_{33}$ (GeV)	1.51	3.55	-3.95
$\tilde{g}_{12}$ (GeV)	0.26	0.20	0.359
$\tilde{g}_{13}$ (GeV)	0.08	0.0535	0.013
$\tilde{g}_{23}$ (GeV)	0.178	0.35	-0.01
$r_1/\tan\beta$	0.0215	0.0247	0.0175
$r_2$	0.191	0.24414	0.159
$r_3$	0.0108	0.006	0.0213
$c_e$	0.355	-3.328	-3.05
$c_\nu$	153.87	45.218	127.0
$\delta m_b$ (GeV)	-24.5	-28.0	-10.25
$\delta V_{cb}$ (GeV)	0.88	0.515	1.07
$\delta V_{ub}$ (GeV)	-0.195	-0.844	-1.0

**Table 2.** Initial values for the model input parameters at the GUT scale with type-I seesaw. Label colors correspond to those in the plots to follow.

We fit to Type-I and type-II seesaw neutrino masses separately and so report the results for each accordingly. Note that throughout the analysis, we take  $v_u = 117.8$  GeV, calculated with  $\tan\beta = 55$  and with  $v_{\text{wk}}$  run to the GUT scale [36].

### 5.0.2 A Note on Threshold Corrections.

Threshold corrections at the SUSY scale are  $\propto \tan\beta$ , and so should be large in this analysis [38]. The most substantial correction is to the bottom quark mass, which is dominated by gluino and chargino loop contributions; this correction also induces changes to the CKM matrix elements involving the third generation. The explicit forms of these corrections can be seen in a previous work on a related model [26]. Additionally, smaller off-diagonal threshold corrections to the third generation parts of  $\mathcal{M}_d$  result in small corrections to the down and strange masses as well as further adjustments to the CKM elements. All such corrections can be parametrized in the model by

$$\mathcal{M}'_d = \mathcal{M}_d + \frac{r_1}{\tan\beta} \begin{pmatrix} 0 & 0 & \delta V_{ub} \\ 0 & 0 & \delta V_{cb} \\ \delta V_{ub} & \delta V_{cb} & \delta m_b \end{pmatrix}, \quad (5.1)$$

where  $\mathcal{M}_d$  is given by eq. (2.2). If we simply take this augmented form for  $\mathcal{M}_d$  as part of the model input, the  $\delta$  parameters can be taken as free parameters, up to some constraints,

which can then aid in the fitting. Their fit values induce constraints on the Higgs and the light stop and sbottom masses. The implications of this implementation were considered in detail for a related model in [26]; in comparing to that work, one can determine for this model that large  $\tan\beta$  and relatively small threshold corrections result in weak and less interesting constraints on the Higgs and squark masses, so we will not consider them further in this analysis.

### 5.1 Fit Results for Type I Seesaw

If one takes  $v_R \lesssim 10^{16}$  GeV and  $v_L \ll 1$  eV, then the type-I contribution is dominant over the type-II contribution, and eq. (2.5) becomes

$$\mathcal{M}_\nu \simeq -\mathcal{M}_{\nu_D} (v_R f)^{-1} (\mathcal{M}_{\nu_D})^T, \quad (5.2)$$

In our initial searches, several similar fermion sector fits were obtained with Dirac phase values of  $\delta_{CP} \sim -65^\circ$ . Table 3 gives the values for the adjusted model input parameters for one example of such a type-I fit, and Table 4 gives the corresponding output values for the fermion parameters. The precise value for the  $\overline{126}$  vev used in this fit is  $v_R = 1.21 \times 10^{15}$  GeV.

To further explore the nature of CP phase in the model, we created scatter plots of sum of chi-squares vs CP phase for the search methods described above in 5.0.1. From the same data, we also made plots of neutrino mixing angles  $\theta_{13}$  and  $\theta_{23}$  vs corresponding phase value. These plots are given in Figures 3 and 4.

We can see from these results that in principle, the model can accommodate virtually any value for the CP phase in the range  $-70^\circ \leq \delta \leq +80^\circ$  while still satisfying all experimental constraints. Closer inspection shows however certain preferred values or ranges, including large negative phases  $-60^\circ \leq \delta \leq -40^\circ$  as well as  $\delta \sim -15^\circ$ . The former is certainly part of a robust region of parameter space, which was explored thoroughly and includes the sample fit given in Tables 3 and 4.

$M$ (GeV)	79.33	$r_1/\tan\beta$	0.023735
$\tilde{f}_{11}$ (GeV)	0.014373	$r_2$	0.2022
$\tilde{f}_{12}$ (GeV)	0.097515	$r_3$	0.0199
$\tilde{f}_{13}$ (GeV)	0.56460	$c_e$	-1.4963
$\tilde{f}_{22}$ (GeV)	1.0219	$c_\nu$	24.317
$\tilde{f}_{23}$ (GeV)	0.0926	$\delta m_b$ (GeV)	-28.00
$\tilde{f}_{33}$ (GeV)	3.85295	$\delta V_{cb}$ (GeV)	-1.495
$\tilde{g}_{12}$ (GeV)	0.26397	$\delta V_{ub}$ (GeV)	0.21557
$\tilde{g}_{13}$ (GeV)	0.22252		
$\tilde{g}_{23}$ (GeV)	1.02642		

**Table 3.** Best-fit values for the model parameters at the GUT scale for a sample model fit with type-I seesaw.

	best fit	exp value		best fit	exp value
$m_u$ (MeV)	0.7246	$0.72^{+0.12}_{-0.15}$	$V_{us}$	0.22427	$0.2243 \pm 0.0016$
$m_c$ (MeV)	208.6	$210.5^{+15.1}_{-21.2}$	$V_{ub}$	0.0030	$0.0032 \pm 0.0005$
$m_t$ (GeV)	80.113	$80.45^{+2.9*}_{-2.6}$	$V_{cb}$	0.03497	$0.0351 \pm 0.0013$
$m_d$ (MeV)	1.515	$0.930 \pm 0.38^*$	$J \times 10^{-5}$	2.29	$2.2 \pm 0.6$
$m_s$ (MeV)	24.47	$17.6^{+4.9*}_{-4.7}$	$\Delta m_{21}^2 / \Delta m_{32}^2$	0.0308	$0.0309 \pm 0.0015$
$m_b$ (GeV)	1.311	$1.24 \pm 0.06^*$	$\theta_{13}$ ( $^\circ$ )	9.397	$8.88 \pm 0.385$
$m_e$ (MeV)	0.3565	$0.3565^{+0.0002}_{-0.001}$	$\theta_{12}$ ( $^\circ$ )	33.62	$33.5 \pm 0.8$
$m_\mu$ (MeV)	75.297	$75.29^{+0.05}_{-0.19}$	$\theta_{23}$ ( $^\circ$ )	43.79	$44.1 \pm 3.06$
$m_\tau$ (GeV)	1.61	$1.63^{+0.04}_{-0.03}$	$\delta_{\text{CP}}$ ( $^\circ$ )	<b>-67</b>	
			$\sum \chi^2$	3.16	

**Table 4.** Best-fit values for the charged fermion masses, solar-to-atmospheric mass squared ratio, and CKM and PMNS mixing parameters for a sample fit with Type-I seesaw. The  $1\sigma$  experimental values are shown [36] (\* - [37]), [28]; masses and mixings are extrapolated to the GUT scale using the MSSM RGEs. Note that the fit values for the bottom quark mass and the CKM mixing parameters involving the third generation shown here include threshold corrections.

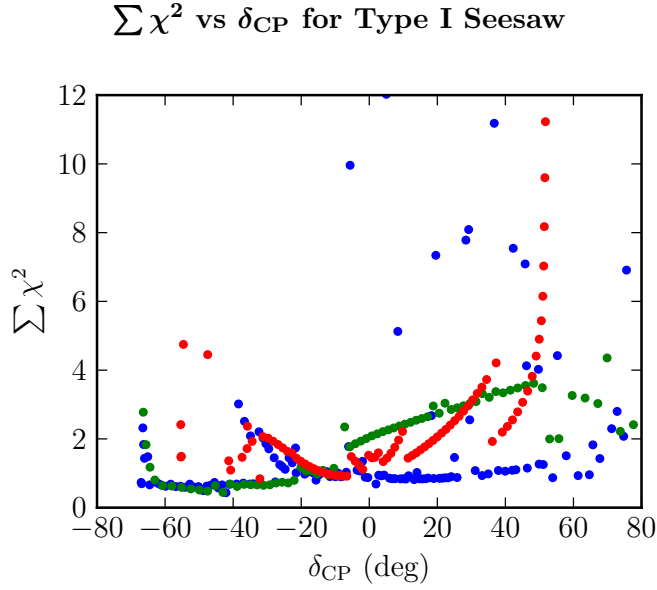


**Figure 3.** Comparisons of the Dirac CP phase angle to sum of chi squares for the model in the type-I seesaw case. Each color represents results for a different set of initial values for the input parameters.

Notably absent is the maximal negative value of  $\sin \delta_{\text{CP}} = -1$ , which may have experimental implications in the coming years.

### Reactor and Atmospheric Angles vs $\delta_{CP}$ for Type I Seesaw

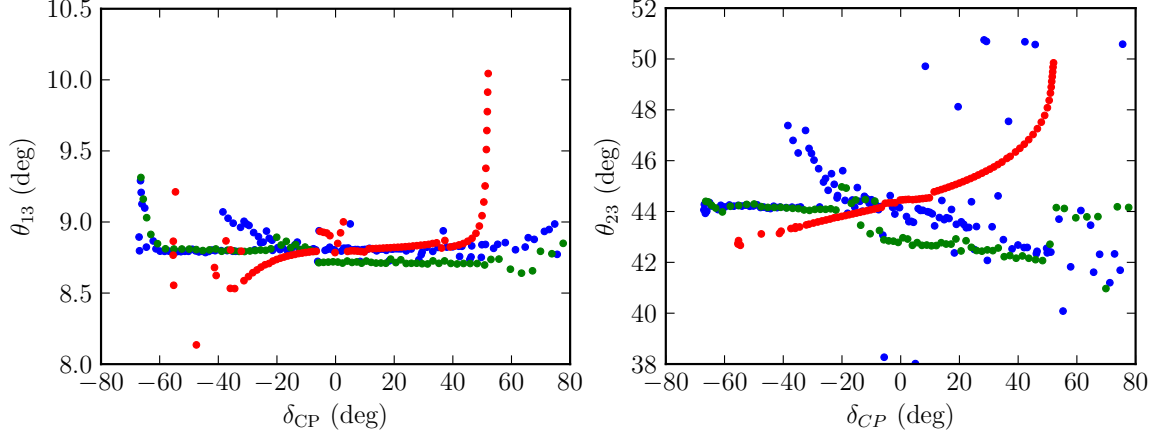


**Figure 4.** Comparisons of the Dirac CP phase angle to neutrino mixing angles  $\theta_{13,23}$  the model in the type-I seesaw case. Each color represents results for a different set of initial values for the input parameters.

#### 5.1.1 Raw Couplings contributing to Proton Decay

In order to calculate the  $C_{ijkl}$  proton decay coefficients, we need the “raw” Yukawa couplings,  $h, f, g$ , which are obtained from the dimensionful couplings,  $\tilde{h}, \tilde{f}, \tilde{g}$ , from the relationships given in eq. (2.3), which are obtained directly from the fit; There is some freedom in the values of the elements of the matrices  $\mathcal{U}, \mathcal{V}$  from the viewpoint of this predominantly phenomenological analysis, but they are constrained by both unitarity and the ratios  $r_i$  and  $c_\ell$ , which have been fixed by the fermion fit. Again, see [17] for details, or see [26] for an example of such a calculation. The resulting dimensionless couplings corresponding to this type-I fit are are

$$h = \begin{pmatrix} 0 & & \\ & 0 & \\ & & 1.6838 \end{pmatrix} \quad f = \begin{pmatrix} 0.00019072 & 0.00129401 & 0.00749214 \\ 0.00129401 & 0.01356053 & 0.00122855 \\ 0.00749214 & 0.00122855 & 0.05112795 \end{pmatrix}$$

$$g = i \begin{pmatrix} 0 & 0.02975586 & 0.02508341 \\ -0.02975586 & 0 & 0.11570158 \\ -0.02508341 & -0.11570158 & 0 \end{pmatrix} \quad (5.3)$$

Here, we see  $f_{11} \sim 0$ , but  $f_{12}, f_{13}$ , and  $g_{12}$  are large enough to seem unfavorable for proton decay. In the end, these factors are suppressed by other means, which we will discuss in Section 6.

#### 5.2 Fit Results for Type II Seesaw

If one takes the  $\overline{126}$  SM-singlet vev  $v_R \gtrsim 10^{17}$  GeV (*i.e.*, the GUT scale), and the triplet vev  $v_L \sim 1$  eV, then the type-II contribution ( $v_L$  term) in eq. (2.5) dominates over the

type-I contribution ( $v_R$  term) by an average of two orders of magnitude in the neutrino mass matrix; therefore eq. (2.5) reduces to

$$\mathcal{M}_\nu \simeq v_L f \quad (5.4)$$

Initial searches here were based on the fit from [18], which gave a small negative CP phase value. Tables 5 and 6 give that fit as a sample here, which uses a precise value for the  $\overline{\Delta}_L$  vev of  $v_L = 1.316 \text{ eV}$ .

$M$ (GeV)	106.6	$r_1/\tan\beta$	0.014601
$f_{11}$ (GeV)	-0.045564	$r_2$	0.0090315
$f_{12}$ (GeV)	0.048871	$r_3$	1.154
$f_{13}$ (GeV)	-0.59148	$c_e$	-2.5342
$f_{22}$ (GeV)	-2.06035	$c_\nu$	n/a
$f_{23}$ (GeV)	-1.4013	$\delta m_b$ (GeV)	-22.740
$f_{33}$ (GeV)	-1.40644	$\delta V_{cb}$ (GeV)	1.2237
$g_{12}$ (GeV)	0.018797	$\delta V_{ub}$ (GeV)	4.2783
$g_{13}$ (GeV)	-0.92510		
$g_{23}$ (GeV)	-3.8353		

**Table 5.** Best fit values for the input parameters at the GUT scale for a sample fit with type-II seesaw (taken from [18]).

Performance of the type II model beyond this point was largely unsuccessful. We were unable to find additional initial values for the input parameters which generated

	best fit	exp value		best fit	exp value
$m_u$ (MeV)	0.7172	$0.72^{+0.12}_{-0.15}$	$V_{us}$	0.2245	$0.2243 \pm 0.0016$
$m_c$ (MeV)	213.8	$210.5^{+15.1}_{-21.2}$	$V_{ub}$	0.00326	$0.0032 \pm 0.0005$
$m_t$ (GeV)	106.8	$95^{+69}_{-21}$	$V_{cb}$	0.0349	$0.0351 \pm 0.0013$
$m_d$ (MeV)	0.8827	$1.5^{+0.4}_{-0.2}$	$J \times 10^{-5}$	2.38	$2.2 \pm 0.6$
$m_s$ (MeV)	34.04	$29.8^{+4.18}_{-4.5}$	$\Delta m_{21}^2/\Delta m_{32}^2$	0.03065	$0.0309 \pm 0.0015$
$m_b$ (GeV)	1.209	$1.42^{+0.48}_{-0.19}$	$\theta_{13}$ ( $^\circ$ )	9.057	$8.88 \pm 0.385$
$m_e$ (MeV)	0.3565	$0.3565^{+0.0002}_{-0.001}$	$\theta_{12}$ ( $^\circ$ )	33.01	$33.5 \pm 0.8$
$m_\mu$ (MeV)	75.297	$75.29^{+0.05}_{-0.19}$	$\theta_{23}$ ( $^\circ$ )	47.70	$44.1 \pm 3.06$
$m_\tau$ (GeV)	1.635	$1.63^{+0.04}_{-0.03}$	$\delta_{\text{CP}}$ ( $^\circ$ )	-7.5	
			$\sum \chi^2$	6.0	

**Table 6.** Best fit values for the charged fermion masses, solar-to-atmospheric mass squared ratio, and CKM and PMNS mixing parameters for a sample fit with Type-II seesaw. The  $1\sigma$  experimental values are also shown for comparison [36], [28], where masses and mixings are extrapolated to the GUT scale using the MSSM renormalization group equations (RGEs). Note that the fit values for the bottom quark mass and the CKM mixing parameters involving the third generation shown here include the SUSY-threshold corrections

significantly different CP phase values. So moving forward with only one initial position in the parameter space, the scatter plots of chi-squares sum vs CP and corresponding plots for the PMNS angles vs CP reveal a bleak situation, which illuminates the difficulty we had in locating different starting points.

The plots in question are given in Figures 5 and 6 below. One quickly notices a much more limited picture of potential phase values. It would seem that the type II model can support small values only for  $\delta_{CP}$ , with best fits (notably superior to the sample fit) giving  $\delta \sim \pm 15^\circ$ .

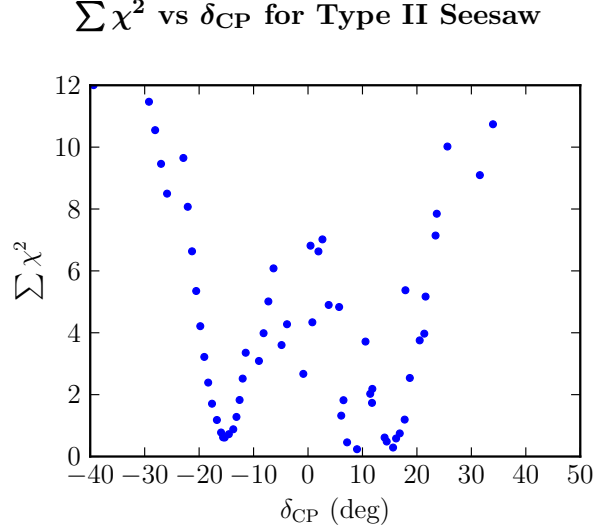


**Figure 5.** Comparisons of the Dirac CP phase angle to sum of chi squares for the model in the type-II seesaw case.

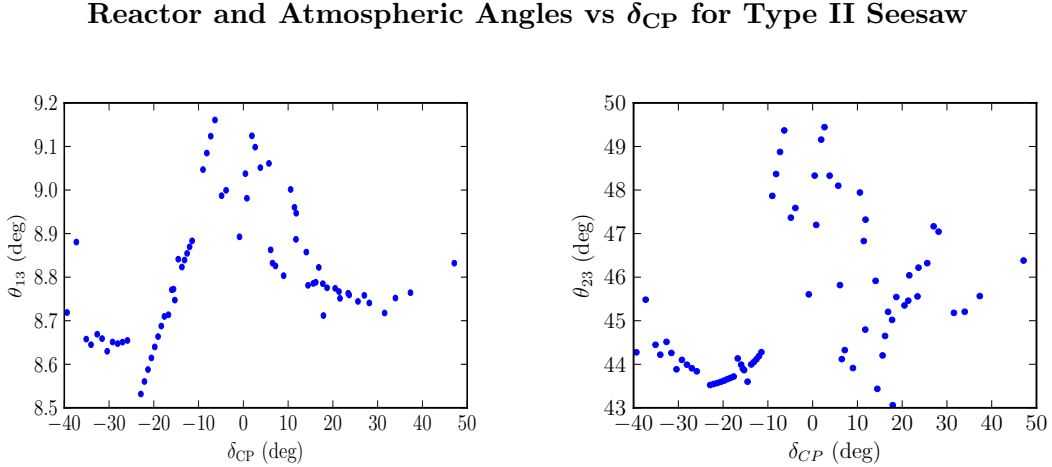


**Figure 6.** Comparisons of the Dirac CP phase angle to neutrino mixing angles  $\theta_{13,23}$  for the model in the type-II seesaw case.

As further evidence for the limitations here, note that the density of the range of  $J_\nu$  values explored on the interval  $[-0.03466, 0.03466]$  was identical to that used in the red and green data for the type-I case. The greatly reduced number of points seen in the plots is the result of numerous minimization attempts failing to converge, as well as additional convergences that gave  $\sum \chi^2 \gtrsim 15$ .

Given the highly limited results of this analysis, we can conclude with statistical confidence that the *type-II-dominant version of this model is unable to accommodate large CP phase values* of either sign, which should result in a *definite fate* for the model as experiments close in on a discovery.

## 6 Proton Lifetime Correlation with Dirac CP Phase

In order to complete this analysis, we now turn to the relationship between CP phase output and the lifetime of the proton. To obtain values for the partial decay widths in consideration, we need values for the  $x_i$  and  $y_i$  triplet mixing parameters found in the  $C_{ijkl}$  operators, in addition to the various SUSY parameters. Recall that the **10** mass parameter  $x_0$  must be  $\mathcal{O}(1)$  to allow the SUSY Higgs fields to be light; the remaining mixing parameters are functions of many undetermined GUT-scale masses and couplings found in the full superpotential, the details of which can be seen in [24]. We simply take the  $x$ s and  $y$ s as the free parameters as discussed above eq. (4.5).

Ideally, one would find that all partial lifetimes are clear of the experimentally determined lower limits, given in Table 7, for arbitrary values  $x, y \in (0, 1)$ , in the absence of unlucky enhancements. It is well-known however that some careful cancellations are required to achieve agreement for a typical GUT model, often of even several orders of magnitude (*e.g.*,  $C^A = -C^B + \mathcal{O}(10^{-3-4})$ ).

The Yukawa textures shown in eq. (3.2) are intended to naturally suppress the values of some crucial  $C_{ijkl}$  elements so that the need for such extreme tuning is alleviated. In [18], we demonstrated that some select but robust regions of parameter space exist among the  $x$ s and  $y$ s that lead to adequate lifetimes in the model for both type-I and II cases, but those results corresponded to a fix CP phase value in each case.

decay mode	$\tau$ exp lower limit (yrs)
$p \rightarrow K^+ \bar{\nu}$	$6.0 \times 10^{33}$
$p \rightarrow K^0 e^+$	$1.0 \times 10^{33}$
$p \rightarrow K^0 \mu^+$	$1.3 \times 10^{33}$
$p \rightarrow \pi^+ \bar{\nu}$	$2.7 \times 10^{32}$
$p \rightarrow \pi^0 e^+$	$1.3 \times 10^{34}$
$p \rightarrow \pi^0 \mu^+$	$1.0 \times 10^{34}$

**Table 7.** Experimentally determined lower limits [39] on the partial lifetimes of dominant proton decay modes considered in this work.

In order to further test the ansatz here, we need to repeat the search for parameter space for multiple fits containing all possible CP phase values, namely the data presented in the previous section. We specifically tested the model by comparing the most constrained  $K^+\bar{\nu}$  mode partial lifetime values to the corresponding CP phase.

The search for such regions was carried out using adaptations of the Python code using `Minuit` described in [18]. Consideration is Results for the type-I and type-II models are reported separately below.

### 6.1 Proton Partial Lifetimes for Type I Seesaw

The resulting scatter plot comparing the  $K^+\bar{\nu}$  mode partial lifetime values to the CP phase values for the type I case is given in Figure 7. The data coloring matches with that used in Section 5 for convenience. One can see that in each case, the fraction of data for which the lifetime is sufficient is on the order of only 20-30%. More interesting is that each of the three initial positions in the parameter space yields a different range of values for  $\delta_{CP}$  for which the model predicts  $K\nu$  lifetimes above the experimental threshold  $6 \times 10^{33}$  yr.

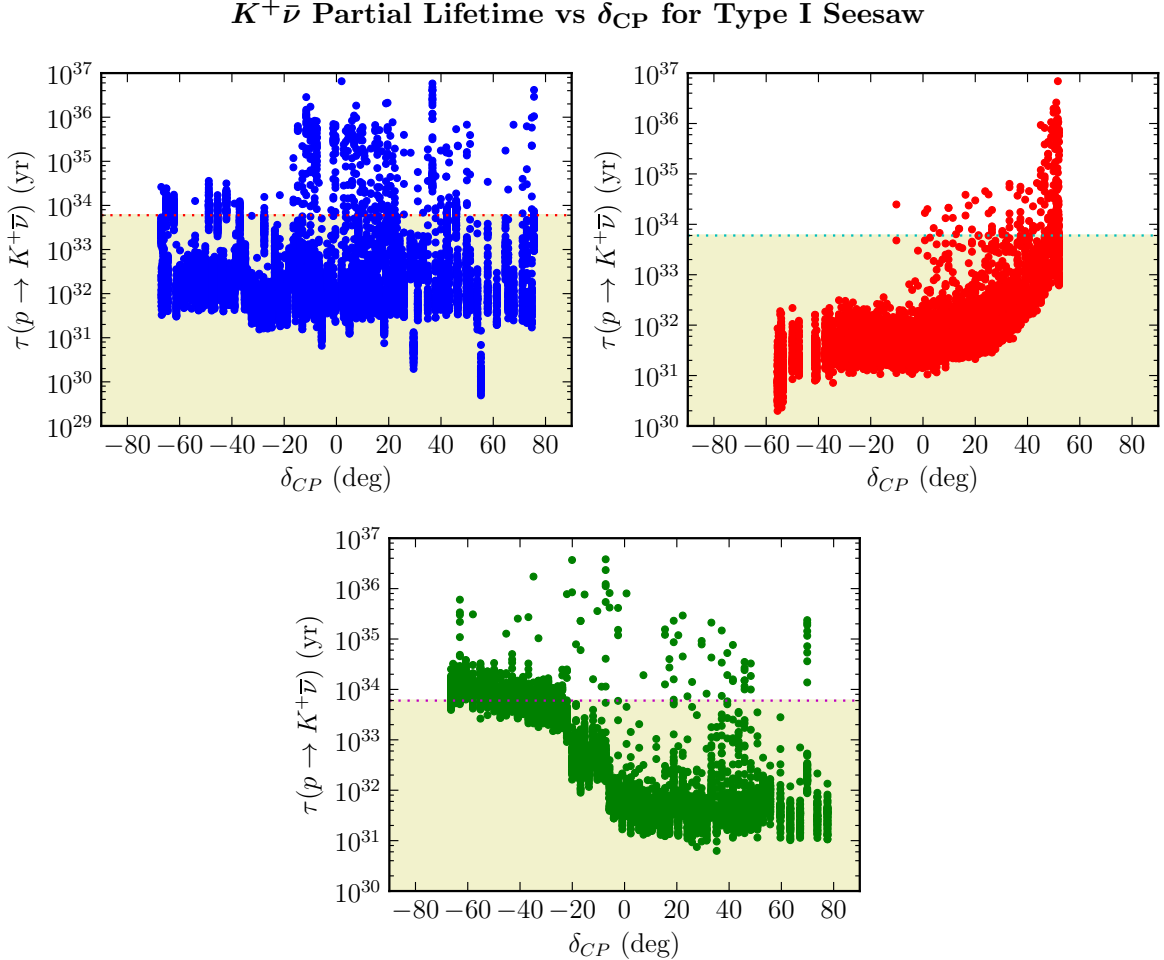


**Figure 7.** Comparisons of the Dirac CP phase angle to the  $K^+\bar{\nu}$  partial lifetime, for the fermion fits discussed above.



Hence it seems that a measurement of the CP phase in the future will select one region as most favorable rather explicitly.

## 6.2 Proton Partial Lifetimes for Type II Seesaw

Despite the heavy constraints put on the Type II case by the fermion sector fitting in Section 5, we report here the corresponding  $K\nu$  lifetime for that data as well. The resulting scatter plot comparing the  $K^+\bar{\nu}$  mode partial lifetime values to the CP phase values for the type II case is given in Figure 8. Here one can see several unfavorable features. First,  $K\nu$  lifetime values for all data are short of the experimental limit (for SUSY breaking scale of 5 TeV). Recall that the analysis in [18], which was more selective in searching for initial positions in the  $x$ - $y$  parameter space, did find a moderately-sized region of parameter space in this model for which the lifetime was adequate, so in that sense, this result is not a complete condemnation of the model; however, that individual fit had  $\delta_{CP} \sim -12^\circ$  and  $\sum \chi^2 \sim 6$ . The second, and more condemning feature of Figure 8 is that the regions of *lowest* lifetime values are those which correspond to the *lowest* chi-square values; hence *sufficient  $K\nu$  lifetime and sufficient fermion fit are in contention with one another*. Finally note that *the only region with feasibly adequate  $K\nu$  lifetime corresponds to  $\delta_{CP} \sim 0$ , i.e., no CP violation in the lepton sector*.

Hence we can further emphasize the imminent failure of the type-II-dominant case determined by this analysis: experimental discovery of any large CP-violating phase in the lepton sector, either positive or negative, will rule out the type-II version of this model. Additionally, any further raising of the experimental limit for the  $K^+\bar{\nu}$  partial lifetime by forthcoming analyses from DUNE, HyperK, T2K, etc would similarly rule out this version of the model if SUSY breaking scale is 5 TeV.

**$K^+\bar{\nu}$  Partial Lifetime vs  $\delta_{CP}$  for Type II Seesaw**

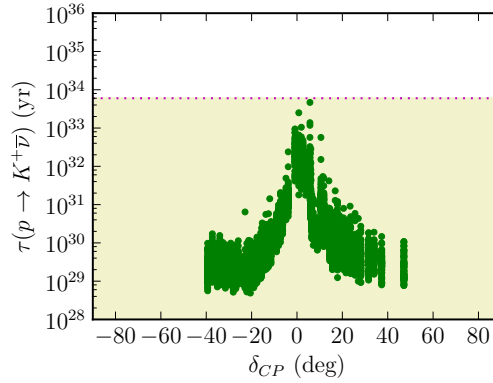


**Figure 8.** Comparisons of the Dirac CP phase angle to the  $K^+\bar{\nu}$  partial lifetime, for the fermion fits discussed above.

## 7 Summary and Conclusion

To summarize, we have considered a renormalizable  $SO(10)$  model that includes a complete and predictive neutrino sector, with seesaw scale emerging from the constraints of coupling unification. This particular model additionally has all fermion masses fit by a specific texture of Yukawa couplings that reduce the fine tuning among different contributions to proton decay.

This model is currently of specific interest because it can be tested by coming experiments designed to measure leptonic CP violation as well as those to measure proton decay. It is particularly interesting that for the current limits on proton lifetime, this model allows a supersymmetry breaking scale in the low-TeV range, which can be tested at the LHC and hadron colliders being planned. Thus our analysis here explored the predictions of the model pertaining to the Dirac CP phase and proton lifetime.

In the Type I seesaw case, we find a robust fermion sector which can support nearly any value for the Dirac CP phase; additionally we find a correlation between the phase value and partial lifetime for the proton decay mode  $p \rightarrow K^+ \bar{\nu}$  that will allow the parameter space of the model to be reduced if measurements for these observables emerge.

In contrast, we find that possible phase values for the Type II case are strongly limited to small values only, and that phase correlation with  $K^+ \bar{\nu}$  partial lifetime further restricts the model into nearly vanishing regions of parameter space. Any discovery of leptonic CP violation or observed increase in proton partial lifetime limits will rule out the Type-II-dominant mode of the model.

Finally, we have suggested that this general class of models with  $\mathbf{10} \oplus \overline{\mathbf{126}} \oplus \mathbf{120}$  (without any specific Yukawa textures) has the potential to solve the strong CP problem without the need for an axion. This makes this particular class of renormalizable SUSY  $SO(10)$  models of great interest. Note that our solution to strong CP does not seem to work in the absence of supersymmetry. A detailed analysis of this strong CP solution is currently in progress and will be the subject of a forthcoming publication.

## Acknowledgement

One of the authors (R.N.M) would like to thank K. S. Babu for discussions. This work is supported by the US National Science Foundation under Grant No. PHY1620074.

## References

- [1] P. Minkowski, Phys. Lett. **B67**, 421 (1977); T. Yanagida in Workshop on Unified Theories, KEK Report 79-18, p. 95 (1979); M. Gell-Mann, P. Ramond and R. Slansky, Supergravity, p. 315; Amsterdam: North Holland (1979); S. L. Glashow, 1979 Cargese Summer Institute on Quarks and Leptons, p. 687; New York: Plenum (1980); R. N. Mohapatra and G. Senjanovic, Phys. Rev. Lett. **44**, 912 (1980).
- [2] For recent reviews and references to literature, see S. F. King, Prog. Part. Nucl. Phys. **94**, 217 (2017) [arXiv:1701.04413 [hep-ph]]; S. F. King and C. Luhn, Rept. Prog. Phys. **76**, 056201 (2013) [arXiv:1301.1340 [hep-ph]].

- [3] S. Raby, Lect. Notes Phys. **939**, 1 (2017); P. Nath and R. M. Syed, Phys. Scripta **92**, no. 12, 124005 (2017).
- [4] H. Georgi, in: Particles and Fields 1974, ed. C.E. Carlson (AIP, NY, 1975) p. 575.; H. Fritzsch and P. Minkowski, Ann. Phys. **93**, 193 (1975).
- [5] K. S. Babu and R. N. Mohapatra, Phys. Rev. Lett. **70**, 2845 (1993) [hep-ph/9209215].
- [6] T. Fukuyama and N. Okada, JHEP 0211, 011 (2002) [hep-ph/0205066]; B. Bajc, G. Senjanovic and F. Vissani, Phys. Rev. Lett. **90**, 051802 (2003) [hep-ph/0210207]; Phys. Rev. **D 70**, 093002 (2004) [hep-ph/0402140]; H. S. Goh, R. N. Mohapatra and S. -P. Ng, Phys. Lett. **B 570**, 215 (2003) [hep-ph/0303055]; Phys. Rev. **D 68**, 115008 (2003) [hep-ph/0308197]; B. Dutta, Y. Mimura and R. N. Mohapatra, Phys. Rev. **D 69**, 115014 (2004) [hep-ph/0402113]; K. S. Babu and C. Macesanu, Phys. Rev. **D 72**, 115003 (2005) [hep-ph/0505200]; T. Fukuyama, A. Ilakovac, T. Kikuchi, S. Meljanac and N. Okada, Eur. Phys. J. C **42**, 191 (2005) [hep-ph/0401213]; Phys. Rev. **D 72**, 051701 (2005) [hep-ph/0412348]; B. Bajc, A. Melfo, G. Senjanovic and F. Vissani, Phys. Rev. **D 70**, 035007 (2004) [hep-ph/0402122]; Phys. Lett. **B 634**, 272 (2006) [hep-ph/0511352]; C. S. Aulakh and A. Girdhar, Nucl. Phys. **B 711**, 275 (2005) [hep-ph/0405074]; T. Fukuyama, A. Ilakovac, T. Kikuchi, S. Meljanac and N. Okada, J. Math. Phys. **46**, 033505 (2005) [hep-ph/0405300]; S. Bertolini, T. Schwetz and M. Malinsky, Phys. Rev. **D 73**, 115012 (2006) [hep-ph/0605006].
- [7] B. Dutta, Y. Mimura and R. N. Mohapatra, Phys. Lett. B **603**, 35 (2004) [hep-ph/0406262]; S. Bertolini, M. Frigerio and M. Malinsky, Phys. Rev. D **70**, 095002 (2004) [hep-ph/0406117].
- [8] W. Grimus and H. Kuhbock, Eur. Phys. J. C **51**, 721 (2007) doi:10.1140/epjc/s10052-007-0324-5 [hep-ph/0612132]; W. Grimus and H. Kuhbock, Phys. Lett. B **643**, 182 (2006) [hep-ph/0607197].
- [9] R. N. Mohapatra, Phys. Rev. D **34**, 3457 (1986); A. Font, L. E. Ibanez and F. Quevedo, Phys. Lett. B **228**, 79 (1989); S. P. Martin, Phys. Rev. D **46**, R2769 (1992).
- [10] C.S. Aulakh and R.N. Mohapatra, Phys. Rev. **D28**, 217 (1983); T.E. Clark, T.K.Kuo, and N.Nakagawa, Phys. Lett. **115B**, 26(1982).
- [11] H. S. Goh, R. N. Mohapatra and S. -P. Ng, Phys. Lett. **B 570**, 215 (2003) [hep-ph/0303055]; K. S. Babu and C. Macesanu, Phys. Rev. D **72**, 115003 (2005) [hep-ph/0505200].
- [12] J. Schechter and J. W. F. Valle, Phys. Rev. D **22**, 2227 (1980); G. Lazarides, Q. Shafi and C. Wetterich, Nucl. Phys. B **181**, 287 (1981); R. N. Mohapatra and G. Senjanovic, Phys. Rev. D **23**, 165 (1981).
- [13] B. Bajc, G. Senjanovic and F. Vissani, Phys. Rev. Lett. **90**, 051802 (2003) [hep-ph/0210207]; Phys. Rev. **D 70**, 093002 (2004) [hep-ph/0402140].
- [14] J. C. Pati and A. Salam, Phys. Rev. D **10**, 275 (1974) Erratum: [Phys. Rev. D **11**, 703 (1975)]; H. Georgi and S. L. Glashow, Phys. Rev. Lett. **32**, 438 (1974).
- [15] H. S. Goh, R. N. Mohapatra, S. Nasri and S. P. Ng, Phys. Lett. B **587**, 105 (2004) [hep-ph/0311330]; T. Fukuyama, A. Ilakovac, T. Kikuchi, S. Meljanac and N. Okada, JHEP **0409**, 052 (2004) [hep-ph/0406068]; M. Severson, Phys. Rev. D **92**, no. 9, 095026 (2015) [arXiv:1506.08468 [hep-ph]]; arXiv:1601.06478 [hep-ph]; T. Fukuyama, K. Ichikawa and Y. Mimura, Phys. Lett. B **764**, 114 (2017);
- [16] K. S. Babu, B. Bajc and S. Saad, See talk at the INT workshop on "Neutron-anti-neutron oscillation", October, 2017.

- [17] B. Dutta, Y. Mimura and R. N. Mohapatra, Phys. Rev. Lett. **94**, 091804 (2005) [hep-ph/0412105]; Phys. Rev. **D 72**, 075009 (2005) [hep-ph/0507319].
- [18] M. Severson, Phys. Rev. D **92**, no. 9, 095026 (2015) [arXiv:1506.08468 [hep-ph]].
- [19] P. Adamson *et al.* [NOvA Collaboration], Phys. Rev. Lett. **118**, no. 23, 231801 (2017) [arXiv:1703.03328 [hep-ex]]; K. Abe *et al.* [T2K Collaboration], Phys. Rev. **D 91**, no. 7, 072010 (2015) [arXiv:1502.01550 [hep-ex]].
- [20] R. Acciarri *et al.* (DUNE) (2015), 1512.06148; 1601.02984
- [21] K. Abe *et al.* [T2K Collaboration], Phys.Rev.D 91,no.7, 072010 (2015).
- [22] E. Kearns *et al.* [Hyper-Kamiokande Working Group], arXiv:1309.0184 [hep-ex]; M. Yokoyama [Hyper-Kamiokande Proto Collaboration], arXiv:1705.00306 [hep-ex]; D. R. Hadley [Hyper-K Collaboration], Nucl. Instrum. Meth. A **824**, 630 (2016).
- [23] F. An *et al.* (JUNO Collaboration), J. Phys. G (Nucl. and Part. Phys.) **43**, id. 030401 (2016); A. Giaz [JUNO Collaboration], PoS EPS **-HEP2017**, 108 (2018).
- [24] C. S. Aulakh and S. K. Garg, Nucl. Phys. B **857**, 101 (2012) [arXiv:0807.0917 [hep-ph]]; Z. Y. Chen, D. X. Zhang and X. Z. Bai, Int. J. Mod. Phys. A **32**, no. 36, 1750207 (2017) [arXiv:1707.00580 [hep-ph]].
- [25] M. A. B. Beg and H.-S. Tsao, Phys. Rev. Lett. **41**, 278 (1978); R. N. Mohapatra and G. Senjanovic, Phys. Lett. **79B**, 283 (1978); A. E. Nelson, Phys.Lett. **B136**, 387 (1984); S. M. Barr, Phys.Rev.Lett. **53** 329 (1984); K. S. Babu and R. N. Mohapatra, Phys. Rev. **D 41**, 1286 (1990); S. M. Barr, D. Chang and G. Senjanovic, Phys. Rev. Lett. **67**, 2765 (1991); R. Kuchimanchi, Phys. Rev. Lett. **76**, 3486 (1996) [hep-ph/9511376]; R. N. Mohapatra and A. Rasin, Phys. Rev. Lett. **76**, 3490 (1996) [hep-ph/9511391]; R. N. Mohapatra and A. Rasin, Phys. Rev. **D 54**, 5835 (1996) [hep-ph/9604445]; L. J. Hall and K. Harigaya, arXiv:1803.08119 [hep-ph].
- [26] P. S. Bhupal Dev, B. Dutta, R. N. Mohapatra and M. Severson, Phys. Rev. D **86**, 035002 (2012) doi:10.1103/PhysRevD.86.035002 [arXiv:1202.4012 [hep-ph]].
- [27] A. S. Joshipura and K. M. Patel, Phys. Rev. D **83**, 095002 (2011) [arXiv:1102.5148 [hep-ph]]; F. Buccella, D. Falcone, C. S. Fong, E. Nardi and G. Ricciardi, Phys. Rev. D **86** (2012) 035012 [arXiv:1203.0829 [hep-ph]]; Y. Mambrini, N. Nagata, K. A. Olive, J. Quevillon and J. Zheng, Phys. Rev. D **91**, no. 9, 095010 (2015) [arXiv:1502.06929 [hep-ph]]; K. S. Babu and S. Khan, Phys. Rev. D **92**, no. 7, 075018 (2015) [arXiv:1507.06712 [hep-ph]].
- [28] K.A. Olive *et al.* (Particle Data Group), Chin. Phys. C, **38**, 090001 (2014).
- [29] M. B. Gavela *et al.* Nucl. Phys. **B312**, **2** (1989) 269.
- [30] S. Aoki *et al.* Phys. Rev. **D62**, 014506 (2000), [arXiv:hep-lat/9911026].
- [31] M. Claudson, M. B. Wise, L. J. Hall. Nucl. Phys. **B195** (1982) 297.
- [32] J. F. Donoghue, E. Golowich. Phys. Rev. **D26** (1982) 3092.
- [33] M. Matsumoto, J. Arafune, H. Tanaka, K. Shiraishi. Phys. Rev. **D46** (1992) 3966; J. Hisano, H. Murayama, T. Yanagida. Nucl. Phys. **B402** (1993) 46.
- [34] F. James and M. Roos, Computer Physics Communications. **10** (1975) 343; [http://seal.web.cern.ch/seal/MathLibs/5 10/Minuit2/html/](http://seal.web.cern.ch/seal/MathLibs/5%20Minuit2/html/)
- [35] G. van Rossum and F.L. Drake (eds). Python Reference Manual, Virginia: Python Labs (2001); <http://www.python.org>

- [36] C.R. Das, M.K. Parida. Eur. Phys. Journal **C20** (2001) 121 [arXiv:hep-ph/0010004].
- [37] K. Bora. *Horizon, A Journal of Physics*, **2** (2013) ISSN 2250-0871, [arXiv:1206.5909 [hep-ph]].
- [38] T. Blazek, S. Raby, S. Pokorski. Phys. Rev. **D52**, 4151 (1995) [hep-ph/9504364].
- [39] K. S. Babu *et al.* Report of the Community Summer Study (*Snowmass 2013*), Intensity Frontier – Baryon Number Violation Group, [arXiv:1311.5285 [hep-ph]].
- [40] G. Altarelli, G. Blankenburg, JHEP **1103** (2011) 133, [arXiv:1012.2697 [hep-ph]].